https://doi.org/10.5194/egusphere-2026-4203
Preprint. Discussion started: 28 July 2026

Flux and Radiocarbon Evidence of Urban Carbon Emission Reductions under Climate Mitigation Policies

Dan Liang,[1,2,3,†] Hongxing Zhang,[4,†] Zhenchuan Niu,[1,5,6,7,*] Sen Wang,[2,8] Weijian Zhou,[1,6] Xuxiang Li,[5] Jingjing Jia,[9] Yifan Tao,[9] Guowei Wang,[1,3] Xue Feng,[1,3] Wanyu Liu,[1,10] Zhao Jin,[1] Yongming Han,[1] Xuefeng Lu,[1,6] Jan B. C. Pettersson[11] and Xiangrui Kong[11]

[1] State Key Laboratory of Loess Science, Institute of Earth Environment, Chinese Academy of Sciences, Xi'an 710061, China

[2] College of Urban and Environmental Sciences, Northwest University, Xi'an 710127, China

[3] Xi'an Institute for Innovative Earth Environment Research, Xi'an, China

[4] State Key Laboratory of Regional and Urban Ecology, Research Center for Eco-Environmental Sciences, Chinese Academy of Sciences, Beijing 100085, China

[5] Institute of Global Environmental Change, Xi'an Jiaotong University, Xi'an, 710049, China

[6] Shaanxi Provincial Key Laboratory of Accelerator Mass Spectrometry Technology and Application, Xi'an AMS Center, Xi'an 710061, China

[7] National Observation and Research Station of Regional Ecological Environment Change and Comprehensive Management in the Guanzhong Plain, Shaanxi, China

[8] Shaanxi Xi'an Urban Ecosystem National Observation and Research Station, National Forestry and Grassland Administration, Xi'an 710127, China

[9] State Key Laboratory of Atmospheric Boundary Layer Physics and Atmospheric Chemistry, Institute of Atmospheric Physics, Chinese Academy of Sciences, Beijing, 100029, China

[10] Interdisciplinary Research Center of Earth Science Frontier, Beijing Normal University, Beijing, 100875, China

[11] Department of Chemistry and Molecular Biology, University of Gothenburg, Gothenburg 41390, Sweden

*Correspondence: Zhenchuan Niu (niuzc@ieecas.cn)

† Dan Liang and Hongxing Zhang contributed equally to this work.

https://doi.org/10.5194/egusphere-2026-4203
Preprint. Discussion started: 28 July 2026

Abstract. Urban areas account for the majority of global CO_2 emissions, yet direct observational evidence of emission reductions under climate mitigation policies remains limited. Here we combine eddy covariance measurements with tree-ring radiocarbon (^{14}C) to quantify changes in urban CO_2 emissions and attribute their sources in two megacities, Beijing and Xi'an, from 2020 to 2024. We find that all urban sites remained net carbon sources but exhibited consistent interannual declines in CO_2 fluxes, with the strongest reductions during heating season and traffic peak hours. Compared to 2021, the CO_2 fluxes in Beijing and Xi'an in 2024 reduced by 21.6% (1.1 kg C m^{-2} yr^{-1}) and 41.2% (0.7 kg C m^{-2} yr^{-1}), respectively. Independent constraints from tree-ring ^{14}C reveal a concurrent decrease in fossil fuel-derived CO_2 (CO_{2ff}), demonstrating that the observed emission reductions are primarily driven by declining fossil fuel combustion. Analysis of energy consumption data indicates that these reductions are associated with substitution of coal and petroleum with electricity and natural gas, as well as rapid adoption of new energy vehicles. Our results provide direct observational evidence that urban carbon emissions can decline under climate mitigation policies and highlight the central role of energy system transformation in achieving sustained emission reductions.

https://doi.org/10.5194/egusphere-2026-4203
Preprint. Discussion started: 28 July 2026

1 Introduction

The rapid rise in atmospheric carbon dioxide (CO_2) concentrations in recent decades, driven by large-scale fossil fuel use and land-use changes, has disrupted Earth's energy balance and accelerated global warming (Solomon et al., 2009). Because more than 70% of global CO_2 emissions originate from urban areas, cities are central to climate mitigation efforts (Canadell et al., 2009). Among major emitters, China plays a pivotal role due to its scale and rapid energy transition (McGlade and Ekins, 2015). In 2020, China launched the "dual-carbon" strategy, committing to peak carbon emissions before 2030 and achieve carbon neutrality by 2060 (MFA, PRC, 2020). The policy framework provides a unique opportunity to examine how urban emission patterns evolve under ambitious mitigation targets and what factors drive these changes.

Previous studies in Chinese cities have explored pathways for reducing urban carbon emission, highlighting measures such as stricter environmental regulations and optimization of urban energy structures based on energy statistics and model-based analysis (Hao et al., 2022; Huang et al., 2022; Wang et al., 2024b; Duan and Zhu, 2025). However, assessing the real-world effectiveness of these policies requires direct observational evidences, particularly to disentangle the contributions of fossil fuel and biogenic sources to urban CO_2 emissions.

The eddy covariance (EC) technique is a widely used *in-situ* approach for quantifying CO_2 exchange between the surface and atmosphere (Baldocchi, 2003; Yu et al., 2006), and has been extensively applied across diverse ecosystems, including urban environments (Hirata et al., 2008; Yu et al., 2008; Wen et al., 2010; Ward et al., 2013; Xiao et al., 2014; Ueyama and Ando, 2016; Wei et al., 2021; Xueref-Remy et al., 2023; Wang et al., 2024a; Zhu et al., 2024). EC measurements provide direct

https://doi.org/10.5194/egusphere-2026-4203
Preprint. Discussion started: 28 July 2026

insights into the magnitude, temporal variability, and interannual trends of urban CO_2 fluxes, revealing whether cities act as net carbon sources or sinks (Ward et al., 2013; Xueref-Remy et al., 2023). However, EC alone cannot distinguish the relative contributions of fossil fuel and biological sources to these fluxes. Therefore, an independent tracer is required to quantify fossil fuel CO_2 (CO_{2ff}) and attribute observed change in urban carbon emissions.

Radiocarbon (^{14}C) is a robust tracer for quantifying CO_{2ff}. Given that the formation time of fossil fuels far exceeds the half-life of ^{14}C (5730 ± 40 years), fossil-derived CO_2 is effectively depleted in ^{14}C (Godwin et al., 1962), in contrast to biogenic CO_2 that reflects contemporary atmospheric levels (Turnbull et al., 2016). Trees assimilate atmospheric CO_2 through photosynthesis and preserve its $\Delta^{14}C$ signature in annual growth rings (Rakowski, 2011). Tree-ring $\Delta^{14}C$ time series therefore enable reconstruction of atmospheric CO_{2ff} concentrations and provide an independent constraint on fossil fuel contributions to urban carbon emissions.

Beijing and Xi'an, two megacities with populations exceeding ten million in northern and western China, respectively, are undergoing rapid energy system transformations under the "dual-carbon" strategy. These cities provide representative cases for evaluating how urban CO_2 emissions respond to large-scale mitigation policies and for identifying the underlying driving mechanisms. In this study, we combined EC and tree-ring ^{14}C measurements to investigate urban carbon emissions in Beijing and Xi'an during 2020–2024. Specifically, we aimed to (i) quantify the temporal dynamics of CO_2 emissions under the "dual-carbon" strategy and identify key periods of emission reduction; (ii) constrain fossil fuel contributions using CO_{2ff} derived from tree-ring ^{14}C; and (iii) identify the dominant drivers of emission changes by integrating energy consumption data. Our results provide observation-based

https://doi.org/10.5194/egusphere-2026-4203
Preprint. Discussion started: 28 July 2026

evidence for evaluating urban carbon mitigation strategies and offer insights applicable to other rapidly developing cities worldwide.

2 Methods

2.1 Site description

Beijing, the capital of China and the core city of the Beijing-Tianjin-Hebei region, is located in northern North China Plain, bordered by the Yanshan Mountains to the north and the Taihang Mountains to the west. It has a warm temperate, semi-humid continental monsoon climate with four distinct seasons. The mean annual temperature ranges from 11 to 13 ℃, and the mean annual precipitation is approximately 500–600 mm based on long-term meteorological records (https://www.beijing.gov.cn/).

Xi’an, the core city of Northwest China, is situated in the Guanzhong Basin at the southern margin of the middle reaches of the Yellow River, bordered by the Qinling Mountains to the south and the Loess Plateau to the north. It has a warm temperate, semi-humid continental monsoon climate with pronounced seasonal variability. The mean annual temperature ranges from 13.5 to 16.6°C, and the mean annual precipitation is 506–1007 mm based on climatological statistics from 1991 to 2024 (https://www.xa.gov.cn/).

One CO_2 flux observation site in Beijing is located on a 325 m meteorological tower at the Institute of Atmospheric Physics (IAP), Chinese Academy of Sciences (39.97 °N, 116.37 °E; Figure 1). This site lies in Haidian District within the North Fourth Ring Road, approximately 8 km from Tian’anmen Square, representing a highly urbanized core area with dense population. The surrounding land cover consists of research and education facilities, residential areas, major transportation corridors, and urban green spaces, providing a representative setting for urban carbon

https://doi.org/10.5194/egusphere-2026-4203
Preprint. Discussion started: 28 July 2026

flux measurements. Tree-ring samples was collected at Madian Park, located 1.8 km from the IAP site. Vegetation within the flux footprint is dominated by typical urban greening species in northern China, including deciduous species (*e.g.*, *Populus tomentosa*, *Sophora japonica*, *Ginkgo biloba*, *Forsythia suspensa*) and evergreen species (*e.g.*, *Pinus tabuliformis*, *Platycladus orientalis*, *Pinus bungeana*).

The second CO_2 flux observation site in Beijing is located on the rooftop of an office building at the Research Center for Eco-Environmental Sciences (RCEES), Chinese Academy of Sciences (40.01 °N, 116.35 °E; Figure 1). The site lies within the North Fifth Ring Road and is adjacent to Tsinghua University, Peking University, and other academic and research institutions, representing a high-density urban environment. The surrounding land cover consists primarily of research and educational buildings, residential areas, urban roads, and artificial green spaces. Tree-ring samples were collected at Dongsheng Bajia Country Park, located 1.1 km from the RCEES. Vegetation within the flux footprint is dominated by common urban landscape species, including deciduous types (*e.g.*, *Sophora japonica*, *Ginkgo biloba*, *Koelreuteria paniculata*) and evergreen species (*e.g.*, *Pinus tabuliformis*, *Pinus bungeana*, *Sabina chinensis*).

One CO_2 flux observation site in Xi'an is situated at the Tang City Wall Relics Park (TCWRP; 34.23 °N, 108.89 °E; Figure 1), within the urban core area inside the South Third Ring Road. Population density exceeds 17,000 persons km^{-2} within this area, indicating a highly concentrated urban environment (Seventh National Population Census, 2020). The surrounding land cover consists of residential areas, commercial buildings, major traffic roads, and vegetation, providing a representative setting for urban carbon flux measurements. Tree-ring samples were collected within the TCWRP, approximately 0.1 km from the flux observation site. Vegetation within the

https://doi.org/10.5194/egusphere-2026-4203
Preprint. Discussion started: 28 July 2026

flux footprint includes typical urban greening species, with deciduous trees (*e.g.*, *Amygdalus persica*, *Ginkgo biloba*, *Jasminum nudiflorum*) and evergreen species (*e.g.*, *Pinus bungeana*, *Magnolia grandiflora*, *Osmanthus fragrans*, *Picea* spp., *Cedrus* spp.).

The second CO_2 flux observation site in Xi'an is located at Guanzhong (GZ; 34.07 °N, 108.35 °E; Figure 1), within the National Observation and Research Station of Regional Ecological Environment Change and Comprehensive Management in the Guanzhong Plain, approximately 50 km from downtown Xi'an. The surrounding land cover consists of villages, vegetation and rural roads, representing a typical rural landscape. Vegetation is dominated by deciduous species (*e.g.*, *Ginkgo biloba* and *Davidia involucrate*) and evergreen species (*e.g.*, *Abies* spp., *Taxus chinensis*, and *Pinus tabuliformis*), along with bamboo (*Fargesia qinlingensis*) and farmland. The area is characterized by sparse settlements and extensive vegetation cover, providing a representative setting for CO_2 exchange in rural ecosystem.

No significant land cover changes were observed in Beijing and Xi'an during 2021–2024, as confirmed by analysis of 30 m resolution land cover datasets (Yang et al., 2024) in conjunction with Territorial Space Master Plan (2021–2035) in both cities.

https://doi.org/10.5194/egusphere-2026-4203
Preprint. Discussion started: 28 July 2026

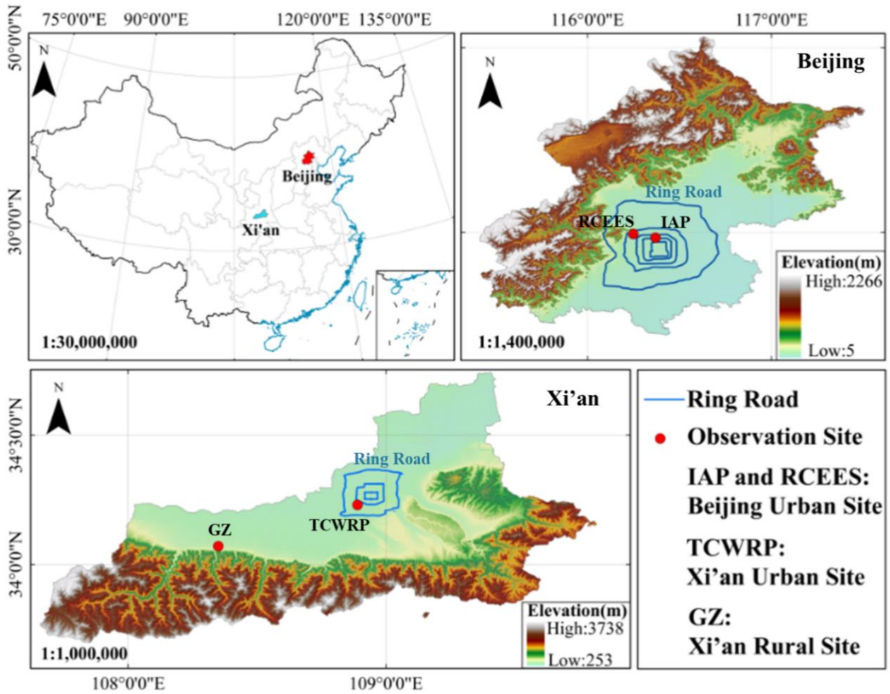

Figure 1. Locations of the observation sites in Beijing and Xi'an, China. The upper-left map shows the positions of Beijing and Xi'an within China. Red dots indicate the observation sites, and blue lines represent the ring roads in each city. IAP, RCEES, TCWRP, and GZ denote the Institute of Atmospheric Physics, the Research Center for Eco-Environmental Sciences, the Tang City Wall Relics Park, and the Guanzhong site, respectively.

2.2 Measurements

CO_2 flux measurements were conducted at the Beijing urban sites (from 1 January 2020 to 30 December 2024), the Xi'an urban site (from 21 January 2021 to 30 December 2024), and the Xi'an rural site (from 16 February 2022 to 30 December 2024). The EC system consisted of an open-path CO_2/H_2O infrared gas analyzer (urban site: LI-7500A; rural site: LI-7500DS; LI-COR Inc., USA) coupled with a three-dimensional ultrasonic anemometer (WindMaster, GILL Inc., UK), installed facing the prevailing wind direction. The analyzers were calibrated every six months using standard CO_2 gases (0 ppm and 395.46 ppm) and a dew-point generator (LI-610,

https://doi.org/10.5194/egusphere-2026-4203
Preprint. Discussion started: 28 July 2026

LI-COR Inc., USA).

At the IAP site, the flux instrument was installed at a height of 140 m on a 325 m iron tower. At the RCEES site, the system was mounted on a 5 m tripod atop a 38 m building, while at the TCWRP site it was mounted at 15 m on a monitoring tower. At the rural GZ site, the instrument was mounted at 20 m on a similar tower. In all cases, the EC system was positioned at more than 1.5 times the mean canopy height of the surrounding vegetation and operated at a sampling frequency of 10 Hz. Signal strength was routinely monitored, and maintenance was performed when it fell below 0.8.

Flux footprint characteristics were determined using the two-dimensional parameterized model of Kljun et al. (2025). For the three urban sites, the dominant land cover types within the 80% flux footprint were buildings, urban roads, and vegetation, with corresponding fetch distances of approximately 4200 m (IAP), 314 m (RCEES), and 200 m (TCWRP) (Figure S1a-c). At the GZ site, the 80% footprint was dominated by villages, rural roads, and vegetation (Figure S1d).

2.3 Data processing and gap-filling

Raw EC data were occasionally lost or corrupted due to adverse weather conditions, power outages, or instrument malfunctions. Pre-processing was therefore applied to ensure data quality and reliability (Amar et al., 2023). The 10 Hz raw data were processed using EddyPro software (LI-COR Inc., USA), including spike removal, time-lag correction, coordinate rotation (double rotation), and ultrasonic virtual temperature correction. The processed high-frequency data were used to compute covariance fluxes, which were then aggregated into 30-minute intervals. The Webb-Pearman-Leuning (WPL) density correction was applied to account for thermal

https://doi.org/10.5194/egusphere-2026-4203
Preprint. Discussion started: 28 July 2026

expansion and water vapor effects, along with frequency response correction for spectral attenuation, yielding CO_2 fluxes at 30-minute resolution.

Quality flags (0, 1, 2) were assigned according to the data quality control method of Foken et al. (2004) Half-hourly CO_2 flux data were excluded if they met any of the following criteria: (1) incomplete datasets (flagged as –9999); (2) quality flag = 2; (3) anomalous negative nighttime flux; (4) fluxes during rainfall events; and (5) stable nighttime conditions with friction velocity (u*) (u* < 0.33 m s^{-1} at the IAP site; u* < 0.16 m s^{-1} at the RCEES site; u* < 0.10 m s^{-1} at the TCWRP site; u* < 0.38 m s^{-1} at the GZ site) (Amiro et al., 2006). Data gaps caused by sensor malfunction, power failure, or quality filtering were filled using the mean diurnal variation (MDV) method (Falge et al., 2001) with a 10-day moving window. All CO_2 fluxes in this study were reported on a carbon mass basis (e.g., g C m^{-2} d^{-1} or mg C m^{-2} h^{-1}).

2.4 Tree-ring sample collection, preparation, and ^{14}C measurement

Tree-ring samples were collected in Beijing and Xi'an in January 2026. The sampled tree species were *Pinus tabuliformis* and *Pinus bungeana*. Core samples were extracted from multiple directions using a 10 mm diameter increment borer, with 2–3 cores collected per tree. The cores were wrapped in clean aluminum foil, and sampling information (time, location, and direction) was recorded.

The samples were air-dried and sanded to clearly distinguish annual rings based on differences between earlywood and latewood under a microscope. Tree rings corresponding to the years 2021–2024 were manually separated and subsequently subjected to organic solvent extraction, bleaching, and alkalization to isolate α-cellulose.

Approximately 3 mg of α-cellulose was mixed with excess wire-shaped copper

https://doi.org/10.5194/egusphere-2026-4203
Preprint. Discussion started: 28 July 2026

oxide and sealed in a 6 mm quartz tube under vacuum (< 10^{-5} torr). The sealed tubes were combusted in a muffle furnace at 850 ℃ for 3 h. The resulting CO_2 was purified in a vacuum line using a liquid nitrogen cold trap (–196 ℃) and an ethanol-liquid nitrogen trap (–90 ℃). The purified CO_2 was then reduced to graphite using the Zn/Fe reduction method (Slota et al., 1987). The graphite was pressed into aluminum targets and analyzed using an accelerator mass spectrometer (0.2 MV MICADAS) at the Xi'an Accelerator Mass Spectrometry Center. The measurement precision was better than 2‰.

The ^{14}C content of a sample is typically expressed as $\Delta^{14}C$, defined as (Stuiver and Polach, 1977):

$$\Delta^{14}C = \left[\frac{(^{14}C/^{12}C)_{SN}}{(^{14}C/^{12}C)_{abs}} - 1\right] \times 1000‰ \quad (1)$$

where $(^{14}C/^{12}C)_{SN}$ is the isotopic ratio in the sample after correction for $\delta^{13}C$-based fractionation and radioactive decay, and $(^{14}C/^{12}C)_{abs}$ is corresponding ratio of the absolute international radiocarbon standard.

2.5 Fossil fuel CO_2 (CO_{2ff}) calculation

CO_{2ff} is typically calculated using the three-source partitioning method, in which ambient atmospheric CO_2 (CO_{2obs}) is divided into three components: background atmospheric CO_2 (CO_{2bg}), CO_{2ff}, and biological CO_2 (CO_{2bio}). Here, Δ_{obs}, Δ_{bg}, Δ_{ff} and Δ_{bio} represent the ^{14}C composition of each component, respectively.

$$CO_{2obs}=CO_{2bg}+CO_{2ff}+CO_{2bio} \quad (2)$$

$$\Delta_{obs}CO_{2obs}=\Delta_{bg}CO_{2bg}+\Delta_{ff}CO_{2ff}+\Delta_{bio}CO_{2bio} \quad (3)$$

The CO_{2bg} concentrations were used as a proxy for CO_{2obs} concentrations, which were not directly available from the tree-ring records.

Combining equations (2) and (3), the formula for calculating CO_{2ff} is as follows:

https://doi.org/10.5194/egusphere-2026-4203
Preprint. Discussion started: 28 July 2026

$$CO_{2ff}=\frac{CO_{2bg}(\Delta_{obs}-\Delta_{bg})}{\Delta_{ff}-\Delta_{obs}}-\frac{CO_{2other}(\Delta_{bio}-\Delta_{obs})}{\Delta_{ff}-\Delta_{obs}} \quad (4)$$

Equation (4) can be simplified by omitting the error term on the right-hand side:

$$CO_{2ff}=\frac{CO_{2bg}(\Delta_{obs}-\Delta_{bg})}{\Delta_{ff}-\Delta_{obs}} \quad (5)$$

Fossil fuels contain no ^{14}C, i.e., $\Delta_{ff} = -1000‰$, since the half-life of ^{14}C is much shorter than the formation time of fossil fuels (Levin et al., 2003). The CO_{2bg} and Δ_{bg} required for calculating CO_{2ff} were obtained from the annual mean CO_2 concentration data at the Waliguan Observatory (https://gml.noaa.gov/data/data.php?site=WLG) and the Northern Hemisphere Zone 1 (NH-1) atmospheric background $\Delta^{14}C$ data (Hua et al., 2022), respectively. Missing data $\Delta^{14}C$ were supplemented using an annual decrease rate of 4‰.

2.6 Bottom-up statistical aggregation of energy consumption data in Beijing and Xi'an City

To assess the influence of anthropogenic energy consumption on CO_2 fluxes, energy consumption data for Beijing and Xi'an were compiled from official statistical sources.

For Beijing, data for 2020–2024 were obtained from the energy balance sheets reported in the *Beijing Statistical Yearbook* (2021–2025). These datasets include seven terminal energy consumption sectors: (1) agriculture, forestry, animal husbandry, and fishery; (2) industry; (3) construction; (4) transportation, storage, and postal services; (5) wholesale, retail, hospitality, and catering; (6) residential consumption; and (7) others.

For Xi'an, energy consumption data for 2021–2023 were derived from the *Shaanxi Provincial Statistical Yearbooks* and *Xi'an Statistical Yearbooks* (2022–2024). The

https://doi.org/10.5194/egusphere-2026-4203
Preprint. Discussion started: 28 July 2026

Xi'an Statistical Yearbook provides detailed information on transportation activity (*e.g.*, subway network length and passenger turnover), but includes direct energy consumption data only for the industrial sector (coal, oil, natural gas, and electricity).

To construct a comprehensive municipal-level energy inventory for Xi'an, a bottom-up scaling approach was applied following Shan et al. (2017). Provincial-level energy balance data for Shaanxi were disaggregated to the city level using sector-specific conversion factors based on the relative contributions of Xi'an and Shaanxi Province. The sectoral classification is consistent with that used for Beijing. Industrial energy consumption was directly obtained from Xi'an Statistical Yearbooks, while the remaining sectors were estimated using conversion factors (Table S1).

The municipal energy consumption for each sector was calculated as:

$$Index_i = \frac{P_{city}}{P_{province}} \times 100\% \tag{6}$$

where P_{city} and P_{province} represent the relevant activity or energy indicators for Xi'an and Shaanxi Province, respectively.

3 Results and discussion

3.1 Interannual reduction of CO_2 fluxes

Figure 2 shows the daily CO_2 fluxes at the observation sites in Beijing and Xi'an. All urban sites exhibited a pronounced "U-shaped" seasonal pattern, with higher CO_2 fluxes in winter and lower values in summer. This seasonal contrast reflects enhanced emissions during the heating period, combined with reduced photosynthetic uptake under low temperature and light conditions, whereas stronger photosynthesis in summer leads to lower net CO_2 fluxes (Delgado-Balbuena et al., 2013; Park et al., 2019).

Despite differences in magnitude, all urban sites acted as net carbon sources and

https://doi.org/10.5194/egusphere-2026-4203
Preprint. Discussion started: 28 July 2026

displayed clear interannual declines in CO_2 fluxes over the study period (Figure 2a-c). For example, annual net carbon exchange decreased from 2021 to 2024 at both Beijing sites (from 7.2 to 6.1 kg C m^{-2} yr^{-1} at IAP, and from 3.0 to 1.9 kg C m^{-2} yr^{-1} at RCEES), with a similar downward trend observed at the Xi'an urban site (from 1.7 to 1.0 kg C m^{-2} yr^{-1}). Notably, anomalously low CO_2 fluxes occurred during periods affected by COVID-19 restrictions, with reduced values observed in Beijing in 2020 and in Xi'an in 2022 during the strict lockdown period (Figure 2a-c), highlighting the strong influence of anthropogenic activity on urban carbon emissions. In addition, lower CO_2 flux values were recorded during the heavy snow period in Beijing, December 2023 (two snowfall events, 14.7 mm snow water equivalent; https://data.cma.cn/), likely driven by reduced anthropogenic emissions associated with the snowfall.

CO_2 fluxes during the Spring Festival further reveal the impact of human activity on urban carbon dynamics. In 2020, festival CO_2 fluxes in Beijing did not differ significantly from non-holiday winter levels, indicating that pandemic-related restrictions suppressed mobility throughout both periods and masked the typical holiday-related emission reduction. In contrast, from 2021 to 2024, CO_2 fluxes during the Spring Festival were consistently lower than non-holiday winter values at both Beijing sites, with an average reduction of 23.6 ± 18.6% (Figure 2a, b). A similar pattern was observed in Xi'an, where Spring Festival CO_2 fluxes decreased by 28.9 ± 4.7% relative to non-holiday periods (Figure 2c). These consistent reductions demonstrate the substantial impact of holiday-associated population migration and reduced anthropogenic activity on urban carbon emissions (Huang et al., 2012; Liu et al., 2024).

https://doi.org/10.5194/egusphere-2026-4203
Preprint. Discussion started: 28 July 2026

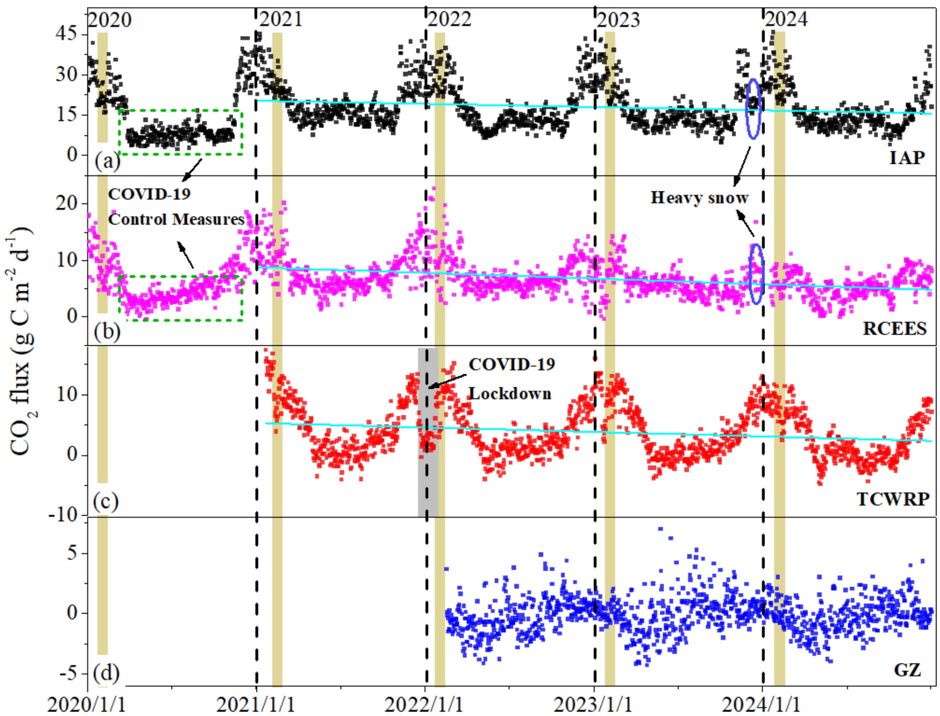

Figure 2. Daily CO_2 fluxes at the observation sites in Beijing and Xi'an. Panels (a) and (b) show the two urban sites in Beijing (IAP and RCEES), while panels (c) and (d) show the urban (TCWRP) and rural (GZ) sites in Xi'an. Yellow shading indicates the Spring Festival period, and gray shading denotes the COVID-19 lockdown period. Green dashed boxes and blue ellipses indicate periods affected by COVID-19 control measures and heavy snow events, respectively. Cyan lines represent linear trends in CO_2 fluxes at the urban sites.

In contrast, the rural site in Xi'an (GZ) functioned as a weak carbon sink or near-neutral system during the observation period, with substantially lower net carbon exchange than the urban sites (Figure 2d). This pattern reflects reduced anthropogenic emissions and greater vegetation influence, with continuous CO_2 uptake by surrounding ecosystems (Havu et al., 2024). The seasonal variability of CO_2 flux was less pronounced than at urban sites, and net carbon uptake occurred throughout most of the year. The strongest sink was observed in spring (March–May), corresponding to the early growing season when increasing temperature enhances photosynthesis while

https://doi.org/10.5194/egusphere-2026-4203
Preprint. Discussion started: 28 July 2026

ecosystem respiration remains relatively low (Davidson et al., 2005).

In contrast to urban sites, CO_2 fluxes at the rural site showed little difference between the Spring Festival and non-holiday periods (Figure 2d), indicating minimal sensitivity to short-term changes in human activity. This suggests that carbon dynamics at the rural site are primarily controlled by natural processes rather than anthropogenic emissions. These findings highlight the contrasting roles of urban and rural environments and underscore the importance of enhancing rural carbon sinks to support low-carbon urban development.

3.2 Further identification of reduction periods of CO_2 fluxes

We further examined the temporal patterns of urban carbon emission reductions by analyzing diurnal variations in CO_2 fluxes (Figure 3). All sites exhibited a clear day-night cycle, reflecting CO_2 release during nighttime and uptake during daytime. At the urban sites in Beijing and Xi'an, CO_2 fluxes showed a pronounced bimodal pattern, with peaks corresponding to morning and evening traffic rush hours (Figure 3a-c), consistent with observations in other cities (Bergeron and Strachan, 2011; Liu et al., 2012).

https://doi.org/10.5194/egusphere-2026-4203
Preprint. Discussion started: 28 July 2026

A clear interannual decline in CO_2 fluxes was observed during the period from November to April (Figure 3a-c), corresponding to the heating season. In particular, hourly CO_2 fluxes at the IAP, RCEES, and TCWRP sites were consistently lower in 2024 compared to 2021 (Figure S2a-c). This seasonal concentration of emission reductions highlights the dominant role of heating-related energy use and its transition toward cleaner energy sources in driving the observed declines.

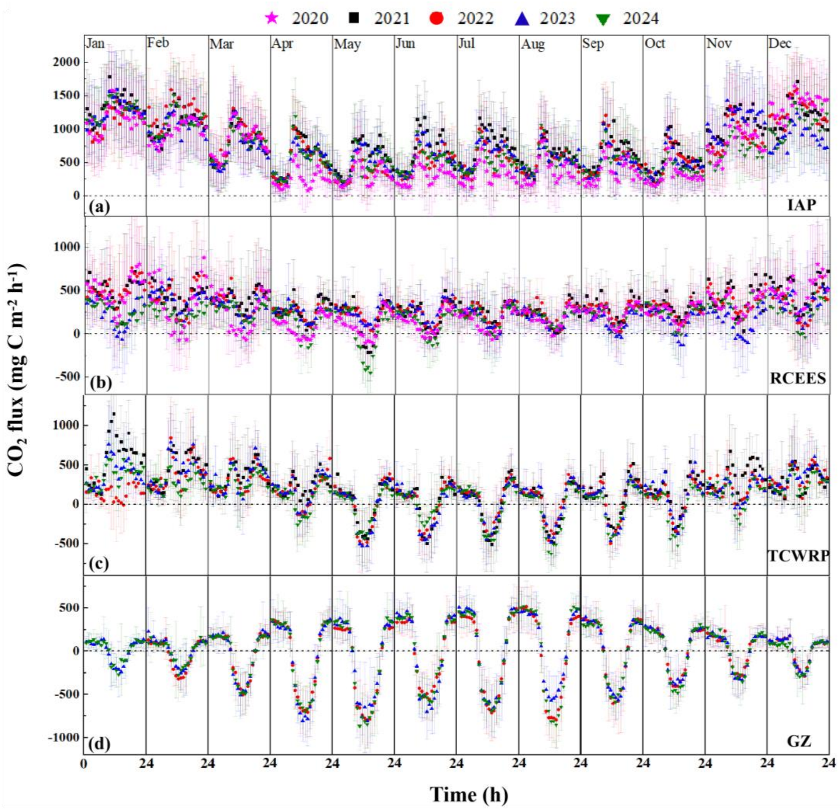

Figure 3. Monthly diurnal variations of CO_2 fluxes at the observation sites in Beijing and Xi'an during 2020–2024. Panels (a) and (b) show the urban sites in Beijing (IAP and RCEES), while panels (c) and (d) show the urban (TCWRP) and rural (GZ) sites in Xi'an.

To identify periods of carbon mitigation, CO_2 fluxes were analyzed separately for heating (November 15–March 15) and non-heating seasons (March 16–November 14).

https://doi.org/10.5194/egusphere-2026-4203
Preprint. Discussion started: 28 July 2026

The corresponding diurnal variations are shown in Figure 4. In Beijing, CO_2 fluxes during the main period of anthropogenic activity (07:00–23:00) reached their lowest levels in 2020, reflecting reduced human mobility during COVID-19 restrictions (Zhao et al., 2025).

During the heating seasons from 2021 to 2024, CO_2 fluxes exhibited a clear interannual decline across all urban sites in both Beijing and Xi'an (Figure 4a, c, e). This decrease was observed throughout the daytime period and was also evident during nighttime hours at the Beijing sites. Notably, the largest reductions occurred during traffic peak hours, indicating a strong contribution from changes in transportation-related emissions.

During the non-heating season, reductions in CO_2 fluxes were also evident, particularly during peak traffic periods (Figure 4b, d, f). These consistent declines across both seasons suggest that emission reductions are not limited to heating-related sources but also reflect broader changes in urban energy use and transportation systems. This pattern is consistent with ongoing energy structure adjustments and the decarbonization of urban transport.

However, interannual variations in summer CO_2 fluxes differed between Beijing and Xi'an, despite the consistent seasonal patterns across all urban sites (Figure 3a-c). In Beijing, summer CO_2 fluxes showed a gradual decline from 2021 to 2024 at both urban sites, whereas no consistent interannual trend was observed at the urban site in Xi'an. This contrast suggests that emission reductions in Beijing extend beyond the heating season, while in Xi'an summer fluxes are more strongly influenced by local variability and non-anthropogenic factors.

At the rural site in Xi'an, CO_2 fluxes exhibited a typical "U-shaped" diurnal cycle, with nighttime CO_2 release driven by ecosystem respiration and daytime uptake

https://doi.org/10.5194/egusphere-2026-4203
Preprint. Discussion started: 28 July 2026

dominated by photosynthesis (Figure 3d) (Zhan et al., 2024). During the growing season (April–September), strong daytime carbon uptake and nighttime release were consistently observed, with no significant interannual differences between 2022 and 2024 (Figure S2d). These patterns indicate that CO_2 fluxes at the rural site are primarily controlled by biogenic processes, with vegetation photosynthesis and ecosystem respiration governing the observed variability.

Although the observation sites in Beijing and Xi'an differ in location, instrument height, spatial footprint, and surface characteristics, a consistent interannual decline in CO_2 fluxes was observed across all urban sites. This decline was evident during both the heating season and peak traffic periods, indicating a robust and systematic reduction in urban carbon emissions.

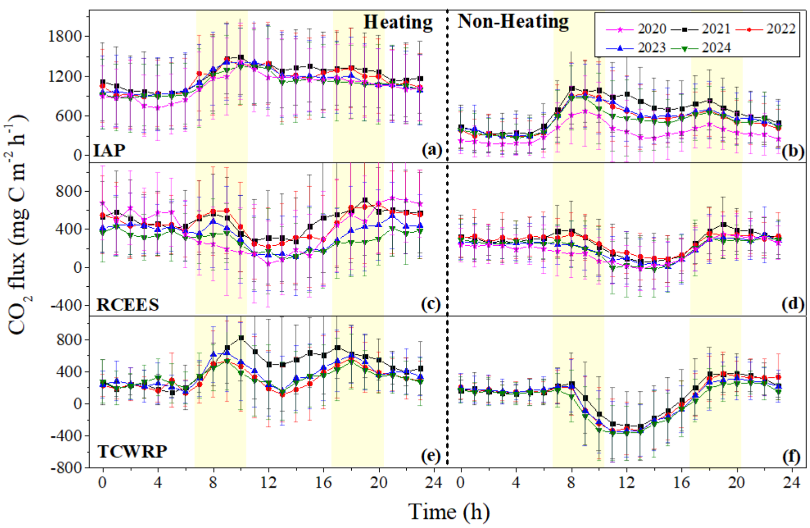

Figure 4. Diurnal variations of CO_2 fluxes at urban sites in Beijing and Xi'an during heating and non-heating seasons. IAP and RCEES represent the Beijing sites, and TCWRP represents the Xi'an site. Yellow shading indicates peak traffic

3.3 Reduction of CO_{2ff} concentrations traced by tree-ring ^{14}C

The interannual decline in CO_2 fluxes observed at the urban sites raises the question

https://doi.org/10.5194/egusphere-2026-4203
Preprint. Discussion started: 28 July 2026

of whether these changes are driven by fossil fuel emissions or biogenic processes. To address this, we analyzed fossil fuel-derived CO_2 (CO_{2ff}) using tree-ring ^{14}C. CO_{2ff} concentrations at all urban sites in Beijing and Xi'an exhibited a clear and consistent decline from 2021 to 2024 (Figure 5). This decrease was observed across all sites, with the largest absolute reduction at the TCWRP site and the lowest overall

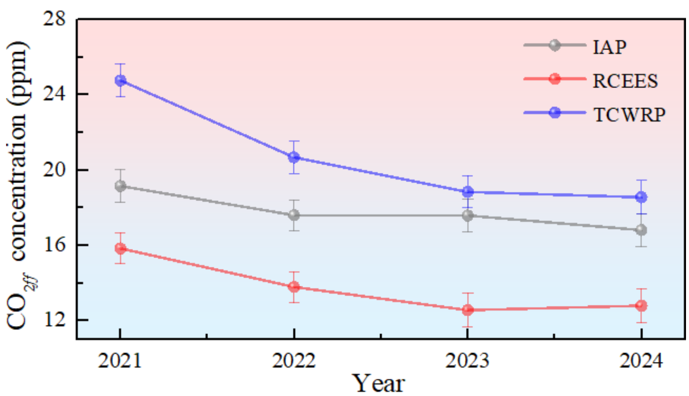

Figure 5. Interannual variations of fossil fuel CO_2 (CO_{2ff}) concentrations based on tree-ring ^{14}C at the urban sites in Beijing and Xi'an from 2021 to 2024.

concentrations at the RCEES site. The consistent downward trends in CO_{2ff} provide direct evidence for a reduction in fossil fuel-derived CO_2 in urban environments.

Further analysis reveals a strong positive correlation between interannual variations in CO_2 fluxes and CO_{2ff} concentrations across the three urban sites. In particular, the IAP site shows an exceptionally high correlation (R^2 = 0.99, p < 0.01), indicating that variations in total CO_2 flux closely track changes in fossil fuel emissions. This strong coupling likely reflects the large footprint of the IAP site, which integrates emissions over a regional scale and is less influenced by local variability. Taken together, the concurrent decline in CO_2 fluxes and CO_{2ff} concentrations demonstrates that reduced fossil fuel combustion is the primary driver of the observed decrease in urban carbon

https://doi.org/10.5194/egusphere-2026-4203
Preprint. Discussion started: 28 July 2026

emissions.

3.4 Analysis of driving factors for the interannual decline in urban CO_2 fluxes using energy consumption data

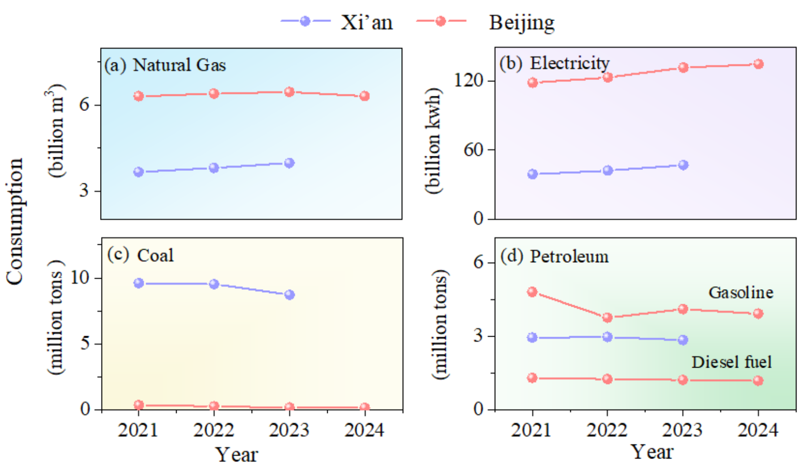

Figure 6. Trends in energy consumption in Beijing (2021–2024) and Xi'an (2021–2023), including (a) natural gas, (b) electricity, (c) coal, and (d) petroleum.

The interannual decline in CO_2 fluxes during the heating season is closely linked to structural changes in urban energy use, as indicated by energy consumption data from both Beijing and Xi'an (Figure 6, S3, S4). Both cities show a clear transition toward cleaner energy, characterized by increasing electricity use and declining coal consumption. This shift, together with a moderate increase in natural gas use, reduces CO_2 emissions associated with heating, as natural gas and electricity have lower carbon intensity than coal (United States Energy Information Administration, 2016). These results suggest that energy structure transformation plays a key role in driving emission reductions during the heating season.

Reductions in CO_2 fluxes during traffic peak periods are associated with changes in transportation systems. Both cities exhibit declining consumption of petroleum-based

https://doi.org/10.5194/egusphere-2026-4203
Preprint. Discussion started: 28 July 2026

fuels and increasing adoption of low-carbon mobility options. In particular, the rapid expansion of metro networks and the large-scale deployment of new energy vehicles (NEVs) indicate a transition toward electrified and public transport systems. Particularly in terms of NEVs, Beijing's fleet size reached over 1 million units in 2024 (a 97.2% increase compared to 2021), and Xi'an's exceeded 400,000 units (a 268.7% rise compared to 2021). These changes are consistent with the observed reductions in CO_2 fluxes during peak traffic hours, highlighting the importance of transport decarbonization in urban emission reductions.

Together with the observed decline in fossil fuel-derived CO_2 (CO_{2ff}), these results demonstrate that reduced fossil fuel combustion is the primary driver of decreasing urban carbon emissions. More broadly, the findings indicate that sustained emission reductions in urban environments are driven by structural transitions in energy and transportation systems, rather than by short-term variability.

4 Conclusions

In summary, this study quantified the temporal evolution and driving mechanisms of urban CO_2 fluxes in Beijing and Xi'an from 2020 to 2024 using eddy covariance measurements combined with tree-ring ^{14}C. Urban sites in both cities acted as persistent carbon sources but exhibited clear interannual declines in CO_2 fluxes from 2021 to 2024. The most pronounced reductions occurred during the heating season and traffic peak hours, highlighting the dominant influence of anthropogenic activities. In contrast, the rural site in Xi'an functioned as a weak carbon sink with no significant interannual trend. Independent constraints from tree-ring ^{14}C reveal a concurrent decline in CO_{2ff}, demonstrating that reduced fossil fuel combustion is the primary driver of the observed emission decreases. Analysis of energy consumption data

https://doi.org/10.5194/egusphere-2026-4203
Preprint. Discussion started: 28 July 2026

further indicates that these reductions are linked to structural changes in urban energy systems, including the substitution of coal and petroleum with electricity and natural gas, as well as the rapid expansion of low-carbon transportation. Overall, our results provide direct observational evidence that urban carbon emissions can decline under sustained climate mitigation policies. They highlight that energy system transformation and transport decarbonization are central to achieving urban emission reductions, while enhanced rural carbon sinks may provide additional support for low-carbon development.

Data availability. The data that support the findings of this study are available in the Figshare repository (https://figshare.com/s/a019e730251e29032259).

Supplement. The supplement related to this article is available online.

Author contributions. Z.N. conceived the study. Z.N., D.L., H.Z., X.L., J.J., Y.T., G.W. and X.F. collected data. Z.N. and D.L. performed sampling and ^{14}C sample preparation. X.L. performed ^{14}C measurements. Z.N., X.K., S.W., W.Z., W.L., Z.J., Y.H. and J.P. provided valuable discussions. D.L. drafted the paper, which was revised by Z.N., X.K. and J.P.

Competing interests. The contact author has declared that none of the authors has any competing interests.

Acknowledgements. This research was jointly supported by the National Natural

https://doi.org/10.5194/egusphere-2026-4203
Preprint. Discussion started: 28 July 2026

Science Foundation of China (Nos. 42173082 and 42330114), and Natural Science Basic Research Program of Shaanxi (No. 2024JC-JCQN-34).

https://doi.org/10.5194/egusphere-2026-4203
Preprint. Discussion started: 28 July 2026

References

Amar, G., Mamtimin, A., Wang, Y., Wang, Y., Gao, J., Yang, F., Song, M., Aihaiti, A., Wen, C., and Liu, J.: Factors controlling and variations of CO_2 fluxes during the growing season in Gurbantunggut Desert, Ecol. Indic., 154, 110708, https://doi.org/10.1016/j.ecolind.2023.110708, 2023.

Amiro, B. D., Barr, A. G., Black, T. A., Iwashita, H., Kljun, N., McCaughey, J. H., Morgenstern, K., Murayama, S., Nesic, Z., Orchansky, A. L., and Saigusa, N.: Carbon, energy and water fluxes at mature and disturbed forest sites, Saskatchewan, Canada, Agri. Forest Meteorol., 136, 237–251, https://doi.org/10.1016/j.agrformet.2004.11.012, 2006.

Baldocchi, D. D.: Assessing the eddy covariance technique for evaluating carbon dioxide exchange rates of ecosystems: past, present and future, Global Change Biol., 9, 479–492, https://doi.org/10.1046/j.1365-2486.2003.00629.x, 2003.

Bergeron, O. and Strachan, I. B.: CO_2 sources and sinks in urban and suburban areas of a northern mid-latitude city, Atmos. Environ., 45, 1564–1573, https://doi.org/10.1016/j.atmosenv.2010.12.043, 2011.

Canadell, J. G., Ciais, P., Dhakal, S., Le Quéré, C., Patwardhan, A. and Raupach, M. R.: The Global Carbon Cycle 2- the Human Perturbation of the Carbon Cycle, Paris, France. No. 10. UNESCO-SCOPE-UNEP Policy Briefs, http://unesdoc.unesco.org/images/0018/001861/186137e.pdf last access June 2018, 2009.

Davidson, E. A., Richardson, A. D., Savage, K. E. and Hollinger, D. Y.: A distinct seasonal pattern of the ratio of soil respiration to total ecosystem respiration in a spruce-dominated forest, Global Change Biol., 12, 230–239, https://doi.org/10.1111/j.1365-2486.2005.01062.x, 2005.

Delgado-Balbuena, J., Arredondo, J. T., Loescher, H. W., Huber-Sannwald, E., Chavez-Aguilar, G., Luna-Luna, M., and Barretero-Hernandez, R.: Differences in plant cover and species composition of semiarid grassland communities of central Mexico and

https://doi.org/10.5194/egusphere-2026-4203
Preprint. Discussion started: 28 July 2026

its effects on net ecosystem exchange, Biogeosciences, 10, 4673–4690, https://doi.org/10.5194/bg-10-4673-2013, 2013.

Duan, Z. and Zhu, X.: The carbon paradox in urban China: High-quality development under the dual-control policy, Sustain, Cities and Soc., 130, 106585. https://doi.org/10.1016/j.scs.2025.106585, 2025.

Falge, E., Baldocchi, D., Olson, R., Anthoni, P., Aubinet, M., Bernhofer, C., Burba, G., Ceulemans, R., Clement, R., Dolman, H., Granier, A., Gross, P., Grünwald, T., Hollinger, D., Jensen, N., Katul, G., Keronen, P., Kowalski, A., Lai, C. T., Law, B. E., Meyers, T., Moncrieff, J., Moors, E., Munger, J. W., Pilegaard, K., Rannik, Ü., Rebmann, C., Suyker, A., Tenhunen, J., Tu, K., Verma, S., Vesala, T., Wilson, K., and Wofsy, S.: Gap filling strategies for defensible annual sums of net ecosystem exchange, Agr. Forest Meteorol., 107, 43–69, https://doi.org/10.1016/S0168-1923(00)00225-2, 2001.

Foken, T., Göckede, M., Mauder, M., Mahrt, L., Amiro, B. and Munger, W.: Post-Field Data Quality Control. In: Lee, X., Massman, W., Law, B. (eds) Handbook of Micrometeorology, Atmospheric and Oceanographic Sciences Library, 29, 181–208, https://doi.org/10.1007/1-4020-2265-4_9, 2004.

Godwin, H.: Half-life of radiocarbon, Nature, 195, 984, 1962.

Hao, J., Gao, F., Fang, X., Nong, X., Zhang, Y. and Hong, F.: Multi-factor decomposition and multi-scenario prediction decoupling analysis of China's carbon emission under dual carbon goal, Sci. Total Environ., 841, 156788, https://doi.org/10.1016/j.scitotenv.2022.156788, 2022.

Havu, M., Kulmala, L., Lee, H. S., Saranko, O., Soininen, J., Ahongshangbam, J., and Järvi, L.: CO_2 uptake of urban vegetation in a warming Nordic city, Urban For. Urban Gree., 94, 128261, https://doi.org/10.1016/j.ufug.2024.128261, 2024.

Hirata, R., Saigusa, N., Yamamoto, S., Ohtani, Y., Ide, R., Asanuma, J., Gamo, M., Hirano, T., Kondo, H., Kosugi, Y., Li, S., Nakai, Y., Takagi, K., Tani, M., and Wang, H.: Spatial distribution of carbon balance in forest ecosystems across East Asia, Agr. Forest

https://doi.org/10.5194/egusphere-2026-4203
Preprint. Discussion started: 28 July 2026

Meteorol., 148, 761–775, https://doi.org/10.1016/j.agrformet.2007.11.016, 2008.

Hua, Q., Turnbull, J. C., Santos, G. M., Rakowski, A. Z., Ancapichún, S., Pol-Holz, R. D., Hammer, S., Lehman, S. J., Levin, I., Miller, J. B., Palmer, J. G., and Turney, C. S. M.: Atmospheric radiocarbon for the period 1950-2019, Radiocarbon, 64, 723–745, https://doi.org/10.1017/RDC.2021.95, 2022.

Huang, K., Zhuang, G., Lin, Y., Wang, Q., Fu, J. S., Zhang, R., Li, J., Deng, C., and Fu, Q.: Impact of anthropogenic emission on air quality over a megacity-revealed from an intensive atmospheric campaign during the Chinese Spring Festival, Atmos. Chem. Phys., 12, 11631–11645, https://doi.org/10.5194/acp-12-11631-2012, 2012.

Huang, R., Zhang, S. and Wang, P.: Key areas and pathways for carbon emissions reduction in Beijing for the "Dual Carbon" targets, Energ. Policy, 164, 112873, https://doi.org/10.1016/j.enpol.2022.112873, 2022.

Kljun, N., Calanca, P., Rotach, M. W. and Schmid, H. P.: A simple two-dimensional parameterisation for Flux Footprint Prediction (FFP), Geosci. Model Dev., 8, 3695–3713, https://doi.org/10.5194/gmd-8-3695-2015, 2015.

Levin, I., Kromer, B., Schmidt, M. and Sartorius, H.: A novel approach for independent budgeting of fossil fuel CO_2 over Europe by $^{14}CO_2$ observations, Geophys. Res. Lett., 30, 2194, https://doi.org/10.1029/2003GL018477, 2003.

Liu, H., Feng, J., Järvi, L. and Vesala, T.: Four-year (2006–2009) eddy covariance measurements of CO_2 flux over an urban area in Beijing,. Atmos. Chem. Phys., 12, 7881–7892, https://doi.org/10.5194/acp-12-7881-2012, 2012.

Liu, Z., Zeng, N., Han, P., Cai, Q., Yao, B., Wang, P., Quan, W., Tang, W., Liang, Z., Liu, Y., and Cory, M.: Detection of Chinese Spring Festival in Beijing using in-situ CO_2 observations and atmospheric inversion, Atmos. Environ., 325, 120446, https://doi.org/10.1016/j.atmosenv.2024.120446, 2024.

McGlade, C. and Ekins, P.: The geographical distribution of fossil fuels unused when limiting global warming to 2 °C, Nature, 517, 187–190, https://doi.org/10.1038/nature14016, 2015.

https://doi.org/10.5194/egusphere-2026-4203
Preprint. Discussion started: 28 July 2026

MFA, PRC (Ministry of Foreign Affairs of the People's Republic of China). Statement by H.E. Xi Jinping President of the People's Republic of China At the General Debate of the 75th Session of The United Nations General Assembly, https://www.ndrc.gov.cn/wsdwhfz/202111/t20211111_1303691_ext.html, 2020.

Park, T., Chen, C., Macias-Fauria, M., Tømmervik, H., Choi, S., Winkler, A., Bhatt, U. S., Walker, D. A., Piao, S., Brovkin, V., Nemani, R. R., and Myneni, R. B.: Changes in timing of seasonal peak photosynthetic activity in northern ecosystems, Global Change Biol., 25, 2382–2395, https://doi.org/10.1111/gcb.14638, 2019.

Rakowski, A. Z.: Radiocarbon method in monitoring of fossil fuel emission, Geochronometria, 38, 314–324, https://doi.org/10.2478/s13386-011-0044-3, 2011.

Shan, Y., Guan, D., Liu, J., Mi, Z., Liu, Z., Liu, J., Schroeder, H., Cai, B., Chen, Y., Shao, S., and Zhang, Q.: Methodology and applications of city level CO_2 emission accounts in China, J. Clean. Prod., 161, 1215–1225, https://doi.org/10.1016/j.jclepro.2017.06.075, 2017.

Slota, P., Jull, A.T., Linick, T. and Toolin, L.: Preparation of small samples for ^{14}C accelerator targets by catalytic reduction of CO, Radiocarbon, 29, 303–306, https://doi.org/10.1017/S0033822200056988, 1987.

Solomon, S., Plattner, G., Knutti, R. and Friedlingstein, P.: Irreversible climate change due to carbon dioxide emissions, Proc. Natl. Acad. Sci. U. S. A., 106, 1704–1709, https://doi.org/10.1073/pnas.0812721106, 2009.

Stuiver, M. and Polach, H. A.: Discussion reporting of ^{14}C data, Radiocarbon, 19, 355–363, https://doi.org/10.1017/S0033822200003672, 1977.

Turnbull, J. C., Keller, E. D., Norris, M. W. and Wiltshire, R. M.: Independent evaluation of point source fossil fuel CO_2 emissions to better than 10%, Proc. Natl. Acad. Sci. U. S. A., 113, 10287−10291, https://doi.org/10.1073/pnas.1602824113, 2016.

Ueyama, M. and Ando, T.: Diurnal, weekly, seasonal, and spatial variabilities in carbon dioxide flux in different urban landscapes in Sakai, Japan, Atmos. Chem. Phys., 16, 14727–14740, https://doi.org/10.5194/acp-16-14727-2016, 2016.

United States Energy Information Administration (EIA), Carbon Dioxide Emission Coefficients: Carbon Dioxide Emissions Coefficients by Fuel, Department of Energy, Washington D.C, 2016.

Wang, J., Yu, G., Han, L., Yao, Y., Sun, M. and Yan, Z.: Ecosystem carbon exchange across China's coastal wetlands: Spatial patterns, mechanisms, and magnitudes, Agr. Forest Meteorol., 345, 109859, https://doi.org/10.1016/j.agrformet.2023.109859, 2024a.

Wang, P., Huang, G., Li, Y., Liu, Y. and Li, Y.: An ecological input-output CGE model for unveiling CO_2 emission metabolism under China's dual carbon goals, Appl. Energ., 365, 123277, https://doi.org/10.1016/j.apenergy.2024.123277, 2024b.

Ward, H. C., Evans, J. G. and Grimmond, C. S. B.: Multi-season eddy covariance observations of energy, water and carbon fluxes over a suburban area in Swindon, UK, Atmos. Chem. Phys., 13, 4645–4666, https://doi.org/10.5194/acp-13-4645-2013, 2013.

Wei, D., Qi, Y., Ma, Y., Wang, X., Ma, W., Gao, T., Huang, L., Zhao, H., Zhang, J., and Wang, X.: Plant uptake outpaces permafrost and plant carbon loss on the Tibetan Plateau, Proc. Natl. Acad. Sci. U. S. A., 118, e2015283118, https://doi.org/10.1073/pnas.2015283118, 2021.

Wen, X., Wang, H., Wang, J., Yu, G. and Sun, X.: Ecosystem carbon exchanges of a subtropical evergreen coniferous plantation subjected to seasonal drought, 2003–2007, Biogeosciences, 7, 357–369, https://doi.org/10.5194/bg-7-357-2010, 2010.

Xiao, W., Liu, S., Li, H., Xiao, Q., Wang, W., Hu, Z., Hu, C., Gao, Y., Shen, J., Zhao, X., Zhang, M., and Lee, X.: A flux-gradient system for simultaneous measurement of the CH_4, CO_2, and H_2O fluxes at a lake–air interface, Environ. Sci. Technol., 48, 14490–14498, https://doi.org/10.1021/es5033713, 2014.

Xueref-Remy, I., Milne, M., Zoghbi, N., Lelandais, L., Riandet, A., Armengaud, A., Gille, G., Lanzi, L., Oppo, S., Brégonzio-Rozier, L., Blanc, P., Yohia, C., Piazzola, J., and Delmotte, M.: Analysis of atmospheric CO_2 variability in the Marseille city area and the north-west Mediterranean basin at different time scales, Atmos. Environ.: X, 17, 100208, https://doi.org/10.1016/j.aeaoa.2023.100208, 2023.

Yang, J. and Huang, X.: The 30 m Annual Land Cover Datasets and Its Dynamics in China from 1985 to 2024 [Dataset], Zenodo., https://doi.org/10.5281/zenodo.12779975, 2024.

Yu, G., Wen, X., Sun, X., Tanner, B. D., Lee, X. and Chen, J.: Overview of ChinaFLUX and evaluation of its eddy covariance measurement, Agr. Forest Meteorol., 137, 125–137, https://doi.org/10.1016/j.agrformet.2006.02.011, 2006.

Yu, G., Zhang, L., Sun, X., Fu, Y., Wen, X., Wang, Q., Li, S., Ren, C., Song, X., Liu, Y., Han, S., and Yan, J.: Environmental controls over carbon exchange of three forest ecosystems in eastern China, Global Change Biol., 14, 2555–2571, https://doi.org/10.1111/j.1365-2486.2008.01663.x, 2008.

Zhan, Y., Deng, Y., Wang, J., Liu, Q. and Wang, W.: Environmental response characteristics of the carbon and water fluxes above complex urban surfaces of a subtropical megacity in China, Phys. Chem. Earth, 135, 103681, https://doi.org/10.1016/j.pce.2024.103681, 2024.

Zhao, L., Zhang, H., Sun, X., Huang, B., Lu, F., Wang, X., and Ouyang, Z.: Dynamics of urban carbon emissions: A comparative analysis of pre- and post-lockdown through eddy covariance measurements, J. Environ. Sci., 158, 735–747, https://doi.org/10.1016/j.jes.2025.01.023, 2025.

Zhu, N., Wang, J., Luo, D., Wang, X., Shen, C. and Wu, N.: Using eddy covariance observations to determine the carbon sequestration characteristics of subalpine forests in the Qinghai-Tibet Plateau, Biogeosciences, 21, 3509–3522, https://doi.org/10.5194/bg-21-3509-2024, 2024.